Journal of Applied Polymer Science

Miscibility, morphology, structure, and properties of porous cellulose–soy protein isolate hybrid hydrogels

Kaiwen Zheng, Junying Zhang, Jue Cheng
Key Laboratory of Carbon Fiber and Functional Polymers (Beijing University of Chemical Technology), Ministry of Education, Beijing 100029, People's Republic of China
Correspondence to: J. Cheng (E-mail: chengjue@mail.buct.edu.cn)

ABSTRACT: Porous hybrid hydrogels were fabricated by mixing cellulose (CEL) and soy protein isolate (SPI) solutions, followed by crosslinking with epichlorohydrin. Their miscibility, morphology, structure, and properties were investigated by wide-angle X-ray diffraction, thermogravimetric analysis, scanning electron microscopy, dynamic mechanical analysis, rheological measurement, and swelling tests. The results show that CEL performed as a "scaffold" of pore walls and contributed to the good mechanical properties, while SPI performed the role of an "extender" of pore size and was responsible for the high water absorbency. The incorporation of CEL (stiff chains) and SPI (hydrophilic groups) in the hybrid hydrogel constructed the porous structure. This work provides a method for the fabrication of hydrogels with porous structure through the combination of a stiff material as a "scaffold" and a hydrophilic material as an "extender." © 2016 Wiley Periodicals, Inc. J. Appl. Polym. Sci. **2016**, *133*, 43853.

KEYWORDS: cellulose; porous hybrid hydrogels; soy protein isolate

Received 16 January 2016; accepted 26 April 2016
DOI: 10.1002/app.43853

INTRODUCTION

Hydrogels, exciting advanced materials, have drawn much attention owing to their applications in the fields of medicine, nursing care, and sensors.[1] For example, biodegradable hydrogels have significant application as implantable carriers for drug-delivery systems because of their reliable nontoxicity and high responsiveness.[2,3] During the past decades, a few notable research studies on the fabrication of biodegradable hydrogels derived either from synthetic materials such as poly(lactic acid)[4], poly(vinyl alcohol),[5] or natural materials such as chitin[6] and gelatin[7] have been discussed. In addition, some biodegradable hydrogels have been fabricated from the combination of synthetic and natural materials through interpenetrating polymer networks (IPN) or semi-IPN.[8–10] Several works were based on natural products[11] because the incorporation of natural materials can increase the biodegradability, safety, and biocompatibility of these polymers.[12]

Cellulose (CEL), the most abundant natural material on earth,[13] has been considered as an alternative to petroleum material because of its low cost, good renewability, and biodegradability.[14–16] Zhang *et al.* have reported[17,18] that CEL has been successfully dissolved in a NaOH/urea aqueous solution and could be used to prepare CEL films,[19] fibers,[20] carriers,[21] and hydrogels.[22] It has been reported by Chang *et al.*[23] that CEL exhibits a wormlike behavior in the NaOH/urea aqueous system, indicating a stiff character that presents good mechanical properties and is suitable for being a backbone of a hydrogel. Thus, CEL displays better properties than the traditional water-soluble material serving as a hydrogel matrix.[24]

Soy protein isolate (SPI), the highest-output plant protein, has been actively researched as an environmentally friendly material in the fields of plastics,[25] films,[26] fibers,[27] and adhesives.[28] Meanwhile, many people refuse to eat genetically modified organisms (GMO) as their safety remains to be determined. Therefore, a large amount of soy planted by transgenic technology is more suitable for industrial materials than foods, and this circumstance makes it urgent for us to develop useful materials from SPI to avoid waste.[29] Normally, SPI needs modification in order to fabricate useful polymer materials because of its poor water resistance caused by the large number of hydrophilic groups, such as —COOH, in it.[30] However, by acting as the "extender" of pore size in hydrogels, SPI can present its excellent water absorbency.

In this work, we attempted to prepare hybrid hydrogels from CEL as a "scaffold" of pore wall and SPI as an "extender" of pore sizeô. CEL and SPI were dissolved in a NaOH/urea aqueous system to form porous hybrid hydrogels by crosslinking with epichlorohydrin (ECH). ECH performed the role of

© 2016 Wiley Periodicals, Inc.

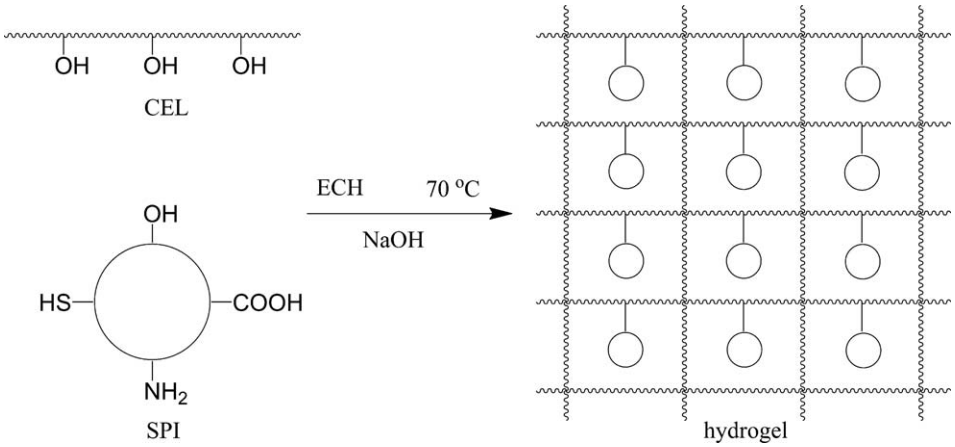

Figure 1. The chemical reaction mechanism and formation process of hydrogel.

crosslinker to connect the hydrophilic groups of CEL and SPI through nucleophilic attack of the alcoholate anion; then a new epoxide formed by the displacement of chloride (Figure 1).[31] To distinguish the different roles of CEL and SPI, the hybrid hydrogels were prepared from a blending of different feedstock ratios. The miscibility, morphology, structure, and properties of the resulting CEL/SPI hybrid hydrogels were investigated by wide-angle X-ray diffraction (WAXD), thermogravimetric analysis (TGA), scanning electron microscopy (SEM), dynamic mechanical analysis (DMA), and rheological measurement. Further, the gelation and swelling behavior of the hydrogels were investigated and discussed in relation to the CEL and SPI content.

EXPERIMENTAL

Materials

Soy protein isolate was purchased from Hubei Yunmeng Technology Co. (China). Cellulose, epichlorohydrin, NaOH, and urea were supplied by Beijing Chemical Reagent Co. (China). The SPI and CEL used in this work were chemically pure (CP), and others were analytically pure (AP). All the chemical reagents were used without further purification.

Preparation of Porous CEL/SPI Hybrid Hydrogels

The CEL/SPI solution was fabricated according to the method reported by Zhang *et al.*[32] after improvement. First, 10 g SPI was dispersed into 162 g water with stirring for 10 min to form a mushy liquid, followed by the addition of 14 g NaOH and 24 g urea. The resulting mixture rapidly turned into a transparent SPI solution after stirring for 5 min and was stored under room temperature. CEL was dispersed in the same solvent (7% NaOH, 12% urea, 81% water) and stored under refrigeration (−15 °C) for 24 h. After that, the frozen solid was taken out for thawing and stirring at room temperature to obtain a transparent CEL solution with a concentration of 4.76 wt %. The SPI and CEL solutions were mixed with varying weight ratios of SPI:CEL of 1:9, 2:8, 3:7, 4:6, and 5:5 and were coded as HG-10, HG-20, HG-30, HG-40, and HG-50, respectively. ECH as crosslinker was added to the mixed solution (1 mL/10 g). The resulting mixtures were stirred at room temperature for another 0.5 h to obtain a homogeneous solution and then gelated at 70 °C for 3 h (using the beaker as support and template). After that, the hybrid hydrogels were fabricated successfully and were taken out carefully to immerse in distilled water to remove the residual chemical reagent for half a month. During this time, the distilled water was replaced twice a day. Finally, the clean hydrogel was kept in distilled water waiting for characterization. The chemical composition and reaction conditions of the resultant hydrogels are summarized in Table I.

Characterization

Wide-angle X-ray diffraction (WAXD) patterns of the samples (CEL, SPI, and HG-50) were recorded on a wide-angle X-ray diffractometer (D/MAX 2500 VB2+/PC, Rigaku Co., Japan) with Cu Kα radiation ($\lambda = 0.154056$ nm) at 40 kV and 200 mA, and the data were collected with 2θ values of 4°–40° at a scanning rate of 1° min^{-1}.

Thermogravimetric analysis (TGA) of the samples (HG-50, the mixture of CEL and SPI, 5 mg) was carried out on a thermogravimetric analyzer (Q-50, TA Co.,) at a heating rate of 10 °C min^{-1} from room temperature to 650 °C under a nitrogen atmosphere.

Scanning electron microscopy (SEM) images of the samples (CEL, HG-10, HG-20, HG-30, HG-40, and HG-50) were recorded on a scanning electron microscope (S-4700, Hitachi Co., Japan). The aerogels, prepared by freeze-drying from hydrogels, were frozen in liquid nitrogen and fractured immediately. The fractured sections of the samples were coated with gold for the SEM observations.

Rheology experiments on the samples (CEL, HG-10, HG-20, HG-30, HG-40, and HG-50) were performed on a rotational rheometer (MCR-101, Anton Paar GmbH, Austria). The mixtures of CEL and SPI solutions with ECH were stirred to form homogeneous solutions. The mixed solutions were quickly transferred into the rheometer for testing. Their elastic storage modulus (E'), viscous loss modulus (E''), and complex viscosity were recorded by a time sweep under a constant shear frequency (1 Hz) at 70 °C.

The compressive stress and the compressive strain of the drenched hydrogels were recorded on a dynamic mechanical analyzer (Q-800, TA Co.). The samples (HG-10, HG-20, HG-30,

Table I. Chemical Composition and Reaction Conditions of the Hybrid Hydrogels

Samples	CEL (4.76 wt %) (g)	SPI (4.76 wt %) (g)	ECH (ml)	Temperature (°C)	Time (h)
HG-10	90	10	10	70	3
HG-20	80	20	10	70	3
HG-30	70	30	10	70	3
HG-40	60	40	10	70	3
HG-50	50	50	10	70	3

HG-40, and HG-50) were cut into a disk shape (diameter-$\times$ height = 10 mm $\times$ 5 mm) and tested in compression mode at room temperature.

The values of equilibrium swelling ratio (ESR) of the hybrid hydrogels (HG-10, HG-20, HG-30, HG-40, and HG-50) were obtained from the formula $ESR = W_1/W_2$, in which W_1 is the weight of the drenched hydrogel at room temperature, and W_2 is that of the dried hydrogel at the same temperature. The hydrogels' weights were found after their surfaces were wiped by filter paper to remove the overflowing water. The final weight of each hydrogel was an average value of three measurements.

To study the rewetting behavior, the dried hydrogels (HG-10, HG-20, HG-30, HG-40, and HG-50) were immersed in distilled water to rehydrate at room temperature. The hydrogels were taken out of the water at regular time intervals to determine their weights. The results are defined as the water absorption (WA) and can be obtained from the formula $WA = (W_t - W_2)/(W_1 - W_2) \times 100\%$, in which W_t is the weight of rewetted hydrogel at time t and the other symbols are as mentioned earlier.

RESULTS AND DISCUSSION

Miscibility, Morphology, and Structure of Hydrogels

Five kinds of CEL/SPI hybrid hydrogels with different feedstock ratios were fabricated successfully, and the photographs of the resulting hydrogels (HG-50 as an example) are given in Figure 2. Obviously, these hydrogels displayed nice appearances like jade, revealing the good miscibility between the two components.

The WAXD patterns of CEL, SPI, and HG-50 are given in Figure 3. The diffraction peaks at $2\theta = 15$, 23, and 34° were assigned to CEL and those at 9° and 19° to SPI. However, HG-50 displayed a completely amorphous state such that the characteristic WAXD peaks of CEL and SPI totally disappeared in it. This result revealed that the chemical crosslinking induced good

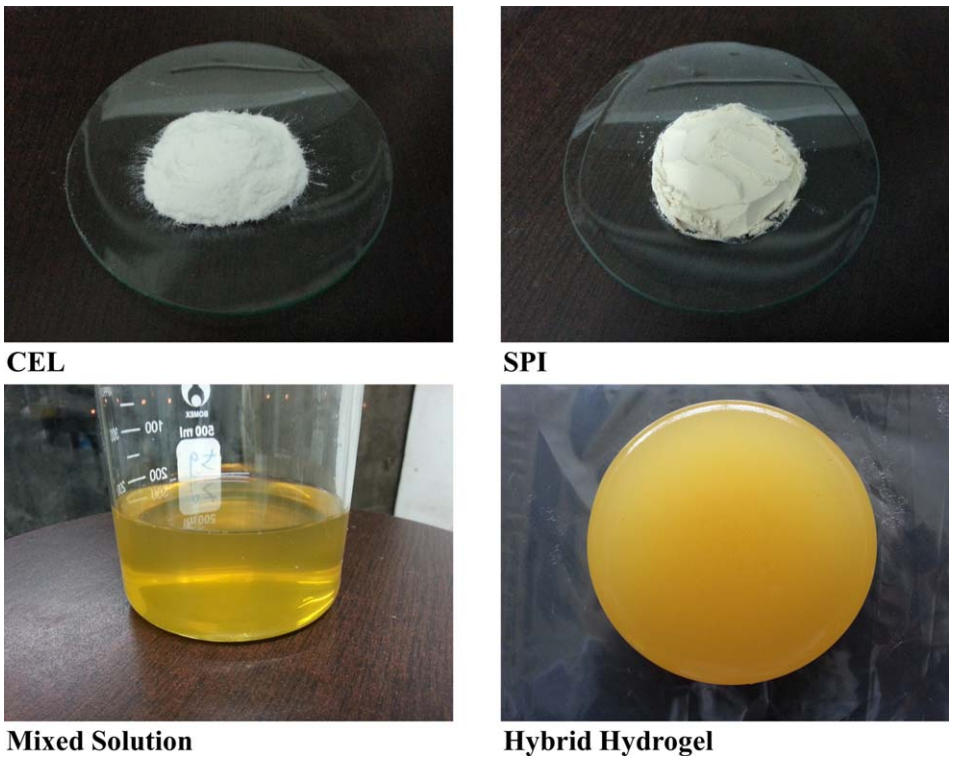

Figure 2. Photographs of CEL, SPI, mixed solution, and hybrid hydrogel. [Color figure can be viewed in the online issue, which is available at wileyonlinelibrary.com.]

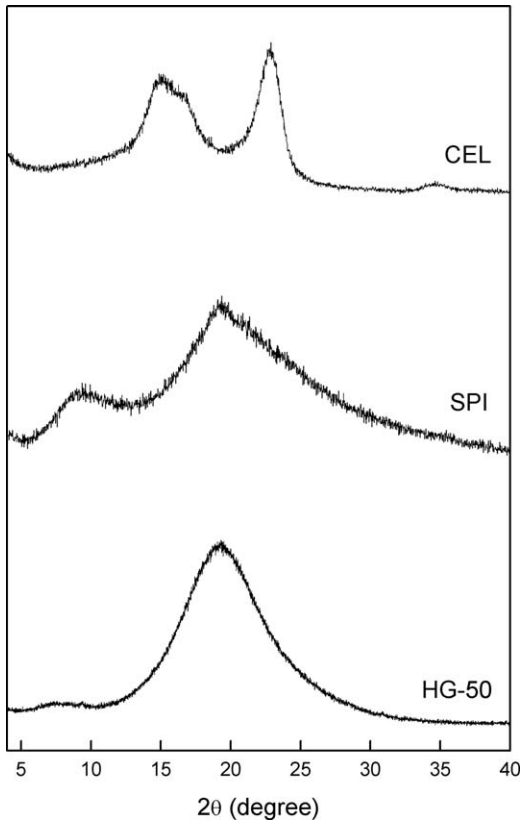

Figure 3. WAXD patterns of CEL, SPI, and HG-50.

miscibility between CEL and SPI and destroyed the original crystalline structure in each component.

TGA is a powerful method for investigating the state of a material and the intermolecular interaction between the two components in a composite system. Figure 4 shows the TGA thermograms of HG-50 and the physical mixture (CEL:SPI = 5:5), while their DTG thermograms are given in Figure 5. The weight loss under 100 °C was due to the removal of residual water from the samples. The physical mixture displayed two evident steps of weight loss,

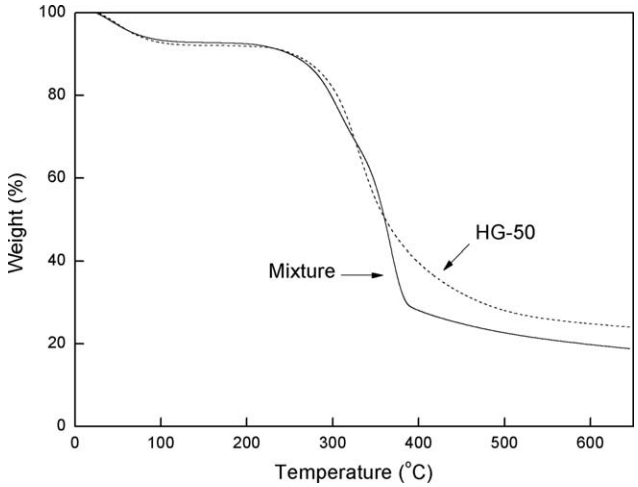

Figure 4. TGA thermograms of HG-50 and the physical mixture (CEL:SPI = 5:5).

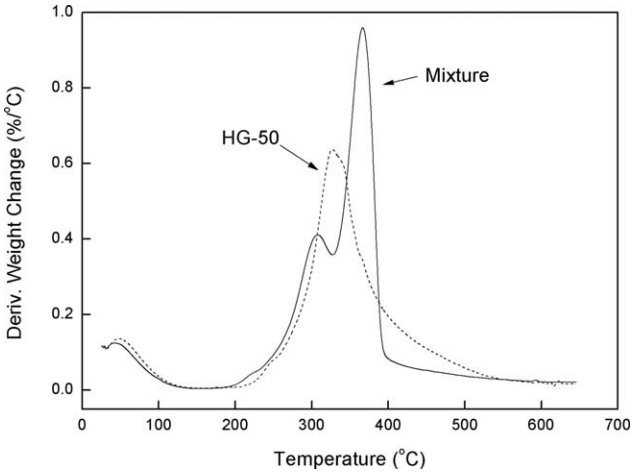

Figure 5. DTG thermograms of HG-50 and the physical mixture (CEL:SPI = 5:5).

which are assigned to CEL and SPI, respectively. The first one from 200 °C to 325 °C was attributed to the decomposition of CEL, while the second one from 325 °C to 400 °C was attributed to the decomposition of SPI. However, there is only one sharp drop from 250 °C to 450 °C in HG-50, which suggested a comparatively high thermal stability and a successful crosslinking occurring in it. Therefore, the results of TGA strongly support the conclusions obtained from WAXD.

Figure 6 presents the interior morphology and structure of the samples. The SEM images suggest that the hydrogels exhibited well-developed, interconnected, and interpenetrated three-dimensional (3D) porous network structures. Obviously, the average pore size of CEL/SPI hybrid hydrogels exceeded 100 μm, which was much bigger than that of the pure CEL hydrogel. This implies that the pore size of the hybrid hydrogel was enhanced with an increase in SPI content. For example, HG-10 displayed a comparatively small pore size with an average of about 60 μm, while HG-50 had a much larger pore size with an average of more than 150 μm. Therefore, it is easy to speculate that the water-absorbing groups in SPI played a significant role in the increase of pore size. Furthermore, these pores had relatively thin pore walls, indicating the tidy arrangement of CEL and SPI. Thus, it was not hard to imagine that the CEL's stiff chains played a significant role in supporting the hydrogel, as the pure SPI hydrogel was too delicate to support by itself. From the results obtained from SEM, we can draw a conclusion that CEL performed as a "scaffold" of the pore wall while SPI acted as an "extender" of the pore size. The blending of CEL (stiff chains) and SPI (water-absorbing groups) resulted in porous hybrid hydrogels. This work provides a method for building a stable porous hydrogel by incorporating both stiff and water-absorbing materials into the network system.

Viscoelastic and Mechanical Properties of Hydrogels

To measure the gelation time of the mixed solutions and the formation process of the resulting hydrogels, a time-sweep measurement for viscoelastic properties was performed on a rheometer at 70 °C. The kinetic curves for storage modulus (E') and loss modulus (E'') of the mixed solutions are presented in

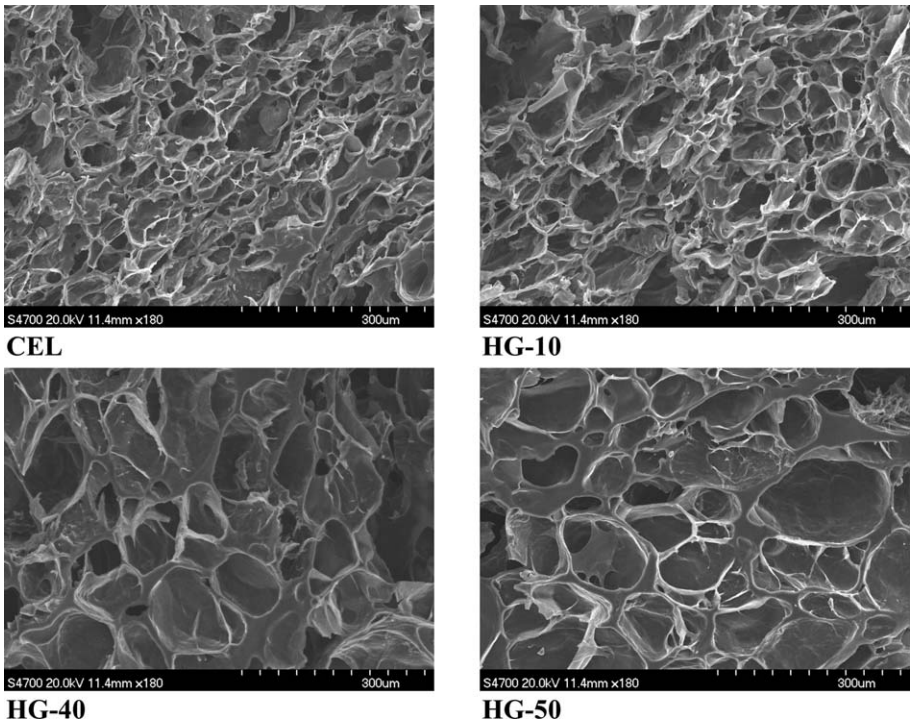

Figure 6. SEM images of CEL, HG-10, HG-40, and HG-50.

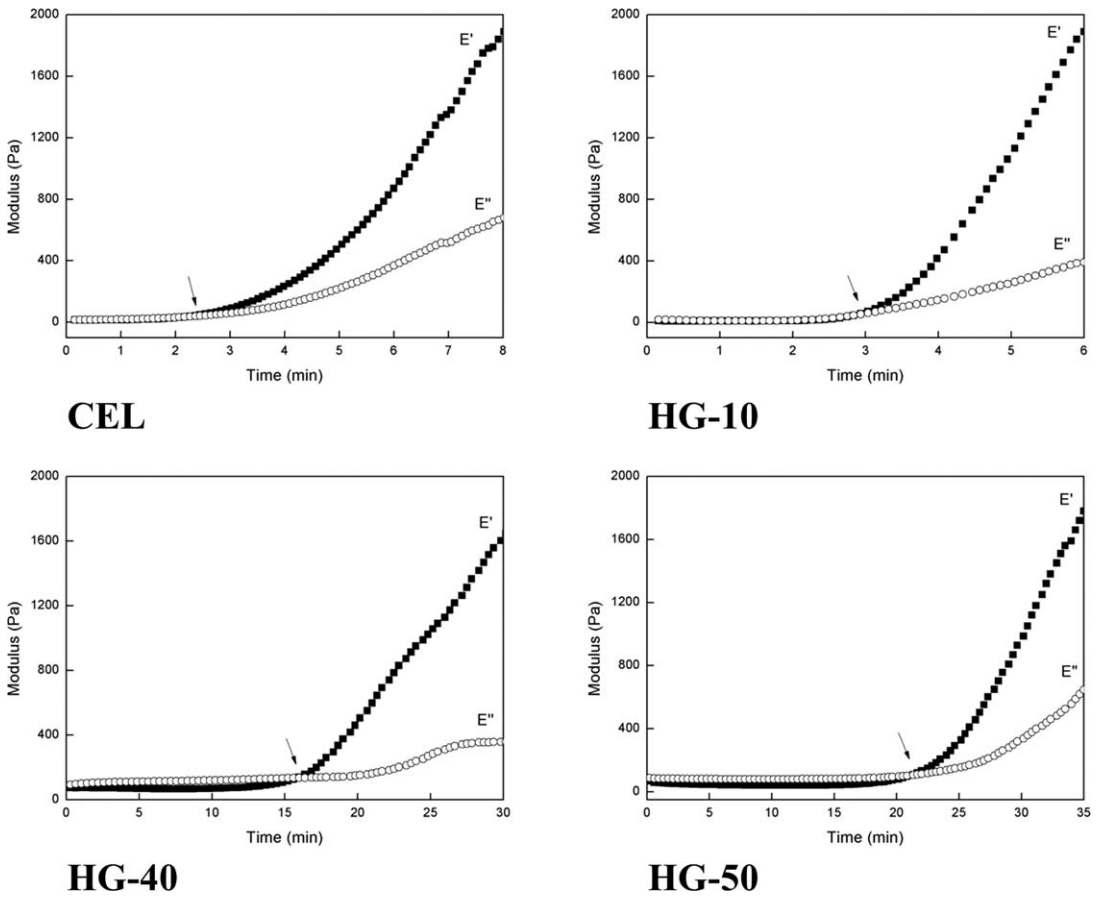

Figure 7. Kinetic curves for storage modulus (E') and loss modulus (E'') of CEL, HG-10, HG-40, and HG-50.

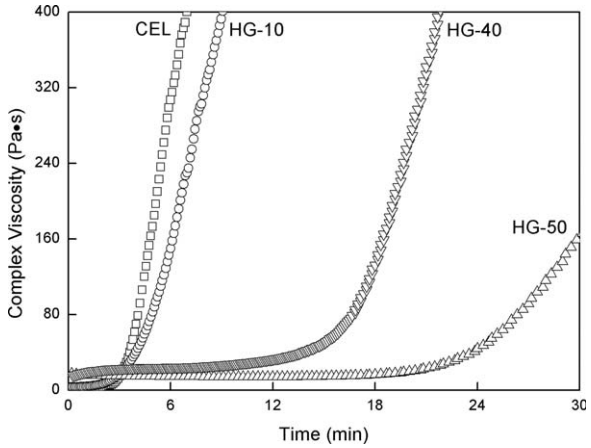

Figure 8. Complex viscosity of CEL, HG-10, HG-40, and HG-50.

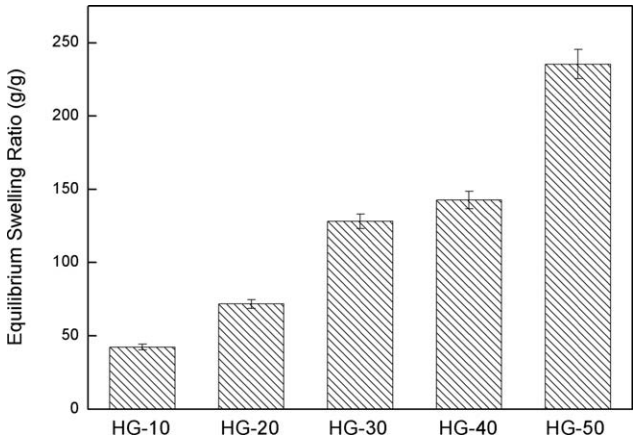

Figure 10. Equilibrium swelling ratio (ESR) of HG-10, HG-20, HG-30, HG-40, and HG-50.

Figure 7 and their complex viscosity in Figure 8. Obviously, all systems displayed a similar gelation behavior. At the beginning, the mixed solutions behaved as viscous liquids, and E' was smaller than E''. Over time, E' increased and finally caught up with E'', and then the mixed solutions became hydrogels. The crossover point ($E' = E''$) is a characteristic in a crosslinking reaction and can be defined as the gel point.[33,34] The gel point can also be measured by the viscosity curves as the viscosity increases with an increase in molecular weight under a constant temperature. The molecular weight of the system increases rapidly near the gel point, therefore leading to the increase of viscosity. Further, the transformation from liquid phase to gel state is owing to the formation of the crosslinking network. In the present case, the gel point of pure CEL hydrogel was about 2.5 min. The gel points of hybrid hydrogels increased from 3 to 21.5 min with a decrease in CEL content, revealing that CEL played an important role in constructing the hydrogel system and mainly contributed to the development of the network system.

The mechanical properties of the hybrid hydrogels were measured by DMA at room temperature, and their compressive stress–strain curves are presented in Figure 9. On one hand, the hybrid hydrogels displayed good mechanical properties, and their stress increased from 12 kPa to 46 kPa with the enhancement of the CEL content in hydrogels. These results strongly agree with the conclusions obtained from SEM analysis that the CEL contributed to supporting the pore wall, leading to the enhancement of the mechanical properties of the hydrogels. On the other hand, the strain of hydrogels increased from 39% to 61% with the increase of SPI content in the hydrogel. However, when the weight ratio of SPI:CEL is higher than 5:5, it is impossible to build a hydrogel as the network is too delicate to stand by itself. Thus, CEL was the matrix of the hydrogel, while SPI could absorb a large amount of water. Moreover, the mechanical properties of the hybrid hydrogels can be controlled by adjusting the content of CEL and SPI to vary their applications.

Swelling Behavior of Hydrogels

The ESR values of the hybrid hydrogels at room temperature are presented in Figure 10. With the feedstock ratio of CEL:SPI dropped from 9:1 to 5:5, the values of ESR were enhanced from 42.3 to 235.4 g/g. The result revealed that the SPI is more

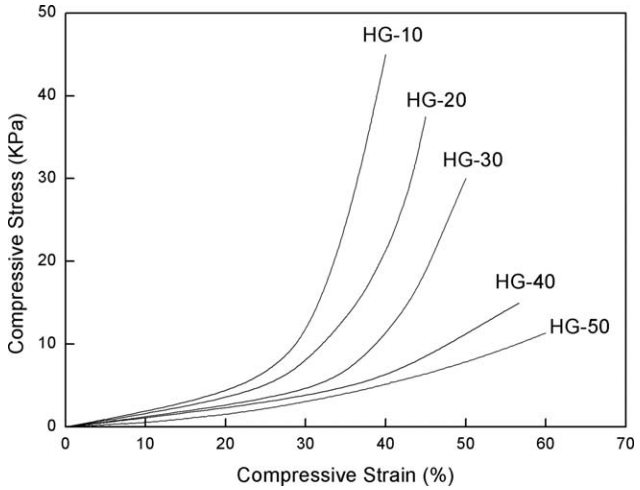

Figure 9. Compressive stress–strain curves of HG-10, HG-20, HG-30, HG-40, and HG-50.

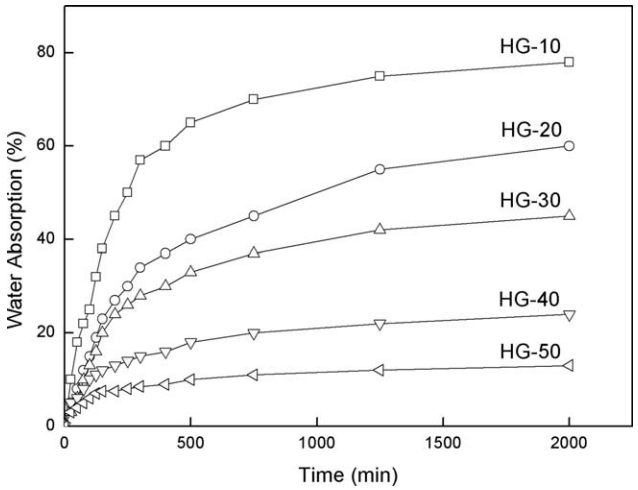

Figure 11. Time-dependent rewetting data of HG-10, HG-20, HG-30, HG-40, and HG-50.

hydrophilic than the CEL and therefore vastly enhanced the hydrophilicity of the hybrid hydrogels. Thus, the ESR results strongly support the conclusion that SPI acted as an "extender" of the pore size.

Figure 11 represents the time-dependent rewetting data. The curves had a typical rewetting pattern, a quick swelling followed by a dilatory and lasting swelling. In detail, all the samples swelled rapidly during the first 500 min; after that, the swelling rates slowed down and finally reached the swelling equilibrium at about 1000–1250 min. Moreover, the water absorption of all hydrogels could not reach 100%, which can be explained by the permanent collapse of the partial network during the vacuum-drying stage. With the feedstock ratio of CEL:SPI dropped from 9:1 to 5:5, the water absorption dropped from 78% to 13%, as the larger and weaker pores collapsed much more easily during the desiccation process.

CONCLUSIONS

Porous hybrid hydrogels were prepared successfully from cellulose and soy protein isolate in a NaOH/urea aqueous solution crosslinked by epichlorohydrin. The resulting hydrogels had high water absorbency and good mechanical properties, which were contributed by SPI and CEL, respectively. The blending of CEL (stiff chains) and SPI (water-absorbing groups) constructed porous hybrid hydrogels. In the hydrogel system, CEL performed as a "scaffold" of the pore wall while SPI acted as an "extender" of the pore size. This work provides a method for the preparation of porous hybrid hydrogels by the blending of stiff and water-absorbing natural products.

ACKNOWLEDGMENTS

The authors greatly appreciated the financial support from the National Natural Science Foundation of China (Project No. 21476013).

REFERENCES

1. Jung, S.; Yi, H. *Chem. Mater.* **2015**, *27*, 3988.
2. Bibian, M.; Mangelschots, J.; Gardiner, J.; Waddington, L.; Diaz Acevedo, M.; De Geest, B.; Van Mele, B.; Madder, A.; Hoogenboom, R.; Ballet, S. *J. Mater. Chem. B* **2015**, *3*, 759.
3. Wu, J.; Chen, A.; Qin, M.; Huang, R.; Zhang, G.; Xue, B.; Wei, J.; Li, Y.; Cao, Y.; Wang, W. *Nanoscale* **2015**, *7*, 1655.
4. Mao, H.; Pan, P.; Shan, G.; Bao, Y. *J. Phys. Chem. B* **2015**, *119*, 6471.
5. Du, G.; Nie, L.; Gao, G.; Sun, Y.; Hou, R.; Zhang, H.; Chen, T.; Fu, J. *ACS Appl. Mater. Interfaces* **2015**, *7*, 3003.
6. He, M.; Wang, Z.; Cao, Y.; Zhao, Y.; Duan, B.; Chen, Y.; Xu, M.; Zhang, L. *Biomacromolecules* **2014**, *15*, 3358.
7. Liang, Y.; Bar-Shir, A.; Song, X.; Gilad, A.; Walczak, P.; Bulte, J. *Biomaterials* **2015**, *42*, 144.
8. Fitzgerald, M.; Bootsma, K.; Berberich, J.; Sparks, J. *Biomacromolecules* **2015**, *16*, 1497.
9. Sharma, K.; Kumar, V.; Kaith, B.; Som, S.; Kumar, V.; Pandey, A.; Kalia, S.; Swart, H. *Ind. Eng. Chem. Res.* **2015**, *54*, 1982.
10. Patwadkar, M.; Gopinath, C.; Badiger, M. *RSC Adv.* **2015**, *5*, 7567.
11. Wang, Q.; Cai, J.; Zhang, L.; Xu, M.; Cheng, H.; Han, C.; Kuga, S.; Xiao, J.; Xiao, R. *J. Mater. Chem. A* **2013**, *1*, 6678.
12. Nair, S.; Zhu, J.; Deng, Y.; Ragauskas, A. *ACS Sustainable Chem. Eng.* **2014**, *2*, 772.
13. Ross, P.; Weinhouse, H.; Aloni, Y.; Michaeli, D.; Weinberger-Ohana, P.; Mayer, R.; Braun, S.; de Vroom, E.; van der Marel, G.; van Boom, J.; Benziman, M. *Nature* **1987**, *325*, 279.
14. Wang, S.; Peng, X.; Zhong, L.; Tan, J.; Jing, S.; Cao, X.; Chen, W.; Liu, C.; Sun, R. *J. Mater. Chem. A* **2015**, *3*, 8772.
15. Hufendiek, A.; Barner-Kowollik, C.; Meier, M. *Polym. Chem.* **2015**, *6*, 2188.
16. Guo, M.; Fei, M.; Liu, H.; Wu, X.; Yang, P. *Polym. Chem.* **2015**, *6*, 2822.
17. Hu, H.; You, J.; Gan, W.; Zhou, J.; Zhang, L. *Polym. Chem.* **2015**, *6*, 3543.
18. Jiang, Z.; Fang, Y.; Xiang, J.; Ma, Y.; Lu, A.; Kang, H.; Huang, Y.; Guo, H.; Liu, R.; Zhang, L. *J. Phys. Chem. B* **2014**, *118*, 10250.
19. Jia, B.; Dong, Y.; Zhou, J.; Zhang, L. *J. Mater. Chem. C* **2014**, *2*, 524.
20. Li, R.; He, M.; Li, T.; Zhang, L. *Carbohydr. Polym.* **2015**, *115*, 269.
21. He, M.; Zhao, Y.; Duan, J.; Wang, Z.; Chen, Y.; Zhang, L. *ACS Appl. Mater. Interfaces* **2014**, *6*, 1872.
22. Li, K.; Song, J.; Xu, M.; Kuga, S.; Zhang, L.; Cai, J. *ACS Appl. Mater. Interfaces* **2014**, *6*, 7204.
23. Chang, C.; He, M.; Zhou, J.; Zhang, L. *Macromolecules* **2011**, *44*, 1642.
24. Zander, N.; Dong, H.; Steele, J.; Grant, J. *ACS Appl. Mater. Interfaces* **2014**, *6*, 18502.
25. Yang, S.; Madbouly, S.; Schrader, J.; Srinivasan, G.; Grewell, D.; McCabe, K.; Kessler, M.; Graves, W. *Green Chem.* **2015**, *17*, 380.
26. Guerrero, P.; Leceta, I.; Peñalba, M.; de la Caba, K. *Mater. Lett.* **2014**, *124*, 286.
27. Salam, A.; Lucia, L.; Jameel, H. *ACS Sustainable Chem. Eng.* **2015**, *3*, 524.
28. Liu, H.; Li, C.; Sun, X. *Ind. Crops Prod.* **2015**, *74*, 577.
29. Zheng, K.; Zhang, J.; Cheng, J. *Ind. Eng. Chem. Res.* **2013**, *52*, 14335.
30. Li, Y.; Chen, F.; Zhang, L.; Yao, Y. *Mater. Lett.* **2015**, *149*, 120.
31. Zhao, W.; Glavas, L.; Odelius, K.; Edlund, U.; Albertsson, A. *Chem. Mater.* **2014**, *26*, 4265.
32. Shi, X.; Hu, Y.; Tu, K.; Zhang, L.; Wang, H.; Xu, J.; Zhang, H.; Li, J.; Wang, X.; Xu, M. *Soft Matter* **2013**, *9*, 10129.
33. Hemp, S.; Smith, A.; Bunyard, W.; Rubinstein, M.; Long, T. *Polymer* **2014**, *55*, 2325.
34. Aufderhorst-Roberts, A.; Frith, W.; Kirkland, M.; Donald, A. *Langmuir* **2014**, *30*, 4483.